Dalton Transactions

PAPER

View Article Online
View Journal

Cite this: DOI: 10.1039/c3dt52081a

Effect of substituent and solvent on cation–π interactions in benzene and borazine: a computational study†

Kusum K. Bania,*[a] Ankur Kanti Guha,*[b] Pradip Kr. Bhattacharyya*[c] and Sourab Sinha[c]

A DFT and *ab initio* quantum chemical study has been carried out at different theoretical levels to delve into the role of the cation–π interaction within the main group metal cations (Li^+, Na^+ and K^+), substituted benzene and borazine. The effects of electron withdrawing and electron donating groups on these non-covalent forces of interaction were also studied. The excellent correlation between Hammett constants and binding energy values indicates that the cation–π interaction is influenced by both inductive and resonance effects. Electron donating groups (EDG) such as $-CH_3$ and $-NH_2$ attached to benzene at the 1, 3 and 5 position and the three boron atoms of borazine were found to strengthen these interactions, while electron withdrawing groups (EWG) such as $-NO_2$ did the reverse. These results were further substantiated by topological analysis using the quantum theory of atoms in molecules (QTAIM). The polarized continuum model (PCM) and the discrete solvation model were used to elucidate the effect of solvation on the cation–π interaction. The size of the cations and the nature of the substituents were found to influence the enthalpy and binding energy of the systems (or complex). In the gas phase, the cation–π interaction was found to be exothermic, whereas in the presence of a polar solvent the interaction was highly endothermic. Thermochemical analysis predicts the presence of thermodynamic driving forces for borazine and benzene substituted with EDG. DFT based reactivity descriptors, such as global hardness (η), chemical potential (μ) and the electrophilicity index (ω) were used to elucidate the effect of the substituent on the reactivity of the cation–π complexes.

Received 1st August 2013,
Accepted 8th October 2013

DOI: 10.1039/c3dt52081a

www.rsc.org/dalton

Introduction

A cation–π interaction is a non-covalent interaction involving aromatic systems. It results from the electrostatic force of attraction between a negative potential generated at the face of the π-system which attracts the cation to its surface.[1–4] This is considered to be one of the weakest forces that occur between alkali metal cations and π-electrons of arene rings.[5] Such weak electrostatic forces of attraction were not well recognized until the pioneering work of Dougherty.[6–8] Later on, execution of important theoretical gas phase studies and the electrostatic model, proposed by Kebarle, established the fundamental features of the cation–π interaction.[9] The strength of the cation–π interaction (similar to Li^+ binding to benzene with 38 kcal mol^{-1} of binding energy and NH_4^+ with 19 kcal mol^{-1}) is also predicted *via* experimental as well as theoretical calculations.[10–12] In recent years, this non-covalent interaction has been recognized as a major force for molecular recognition,[13,14] bringing together the hydrophobic effects, hydrogen bonds, and the ion pairs in determining macromolecular structures and drug–receptor interactions.[15] Many studies have established the importance of the cation–π interaction on numerous biological processes.[16–19] The role of the cation–π interaction in understanding the stereochemistry of chiral molecules has also been well explored in various asymmetric synthesis.[20–22]

It is important to mention herein that to date, many theoretical studies have been performed to understand the fundamental aspects of the cation–π interaction and the strength of such interactions.[23] And in many cases, it is the organic aromatic systems which are of importance as they also play a pivotal role in biological systems.[24] However, less attention has been paid to understanding the nature of such interactions within borazine, the so called "*Inorganic Benzene*".[25,26]

[a]*Tezpur University, Napaam, Assam 784028, India. E-mail: kusum@tezu.ernet.in*
[b]*Dibrugarh University, Dibrugarh, Assam 786004, India.*
E-mail: ankurkantiguha@gmail.com
[c]*Arya Vidyapeeth College, Guwahati, Assam 781016, India.*
E-mail: prdpbhatta@yahoo.com

†Electronic supplementary information (ESI) available: Necessary supplementary figures and tables are provided. See DOI: 10.1039/c3dt52081a

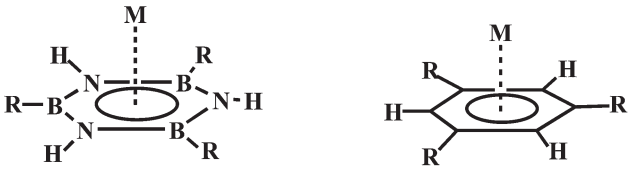

$M = Li^+, Na^+, K^+; R = H, CH_3, NH_2, NO_2$

Scheme 1 Illustration of cation–π interaction in benzene and borazine. R represents the EDG and EWG.

Borazine and benzene are misnomers with similar physical properties and varied chemical properties.[27] The lower aromaticity of borazine and the involvement of electropositive (B) and electronegative (N) atoms make this molecule an attractive target for π-interaction by cations.

There are several important factors which modulate and govern this non-covalent cation–π interaction including, the size of the cations, the solvent and the nature of the substituent. Benzene is used as a prototypical representative for the π group in a majority of the studies. A series of high-accuracy gas-phase computational studies have been performed to understand the cation–π interaction in benzene and in the benzene sandwich dimer.[28–30] G. N. Sastry and his co-workers have reviewed the effects of various factors on the cation–π interaction in various organic aromatic systems.[31] However, such studies of borazine are sparse and thus, herein, we have taken a forward step in investigating the properties of the cation–π interaction within borazine using quantum chemical computations and by performing some topological analysis (Scheme 1). It has been revealed from previous studies that substituents on the B atom of borazine have a dramatic effect on its structure and aromaticity.[32] We have therefore considered both substituted borazine and benzene in our study. In the case of borazine, the electron withdrawing group (EWG, $-NO_2$) and the electron donating groups (EDG, $-CH_3$ and $-NH_2$) are substituted at the B-atom and in the case of benzene, these groups are placed at the 1, 3 and 5 positions, Scheme 1.

Results and discussion

Molecular geometry

Optimized structures of the cation–π complexes of benzene and borazine obtained at the MP2/6-31+G(d) level of theory are shown in Fig. 1 and 2, respectively. Geometrical parameters of the considered systems are provided in Table 1. It can be observed from Table 1 that, the C–C and B–N bonds in the cationic complexes are slightly longer than the free benzene and borazine molecules respectively, consistent with donation of electron density from the ring to the cation.[33] Also, observations made from Table 1 construed that, both the C–C and B–N bond distances were found to be much more elongated as the size of the cations under investigation decreases. On substituting the boron atoms of borazine with a strong electron withdrawing group such as $-NO_2$, the B–N bond length compresses by a factor of ~0.005–0.012 Å. The most profound decrease is observed with a K^+ ion. These observations indicate that the presence of EDGs results in the elongation of either C–C or B–N bond distances whereas the presence of EWGs results in the decrease of the above specified bond lengths. Variation in the C–C and B–N bond lengths in the presence of

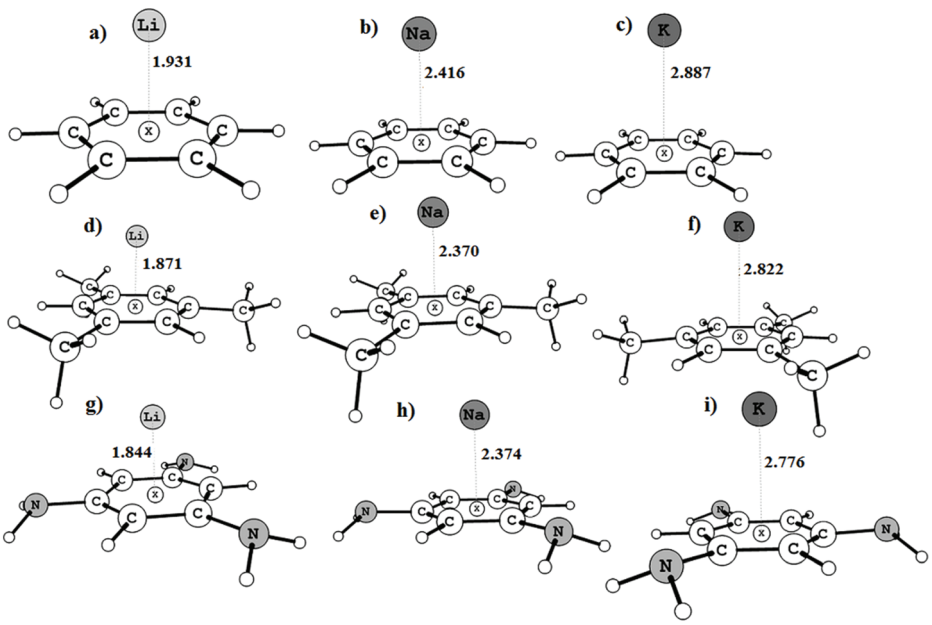

Fig. 1 Optimized geometries at the MP2/6-31+G(d) level of theory of the cation–π complexes of benzene (a–c) and substituted benzene (d–i). Here, X is the geometric mean of the ring and the cation–π distances are in angstrom (Å).

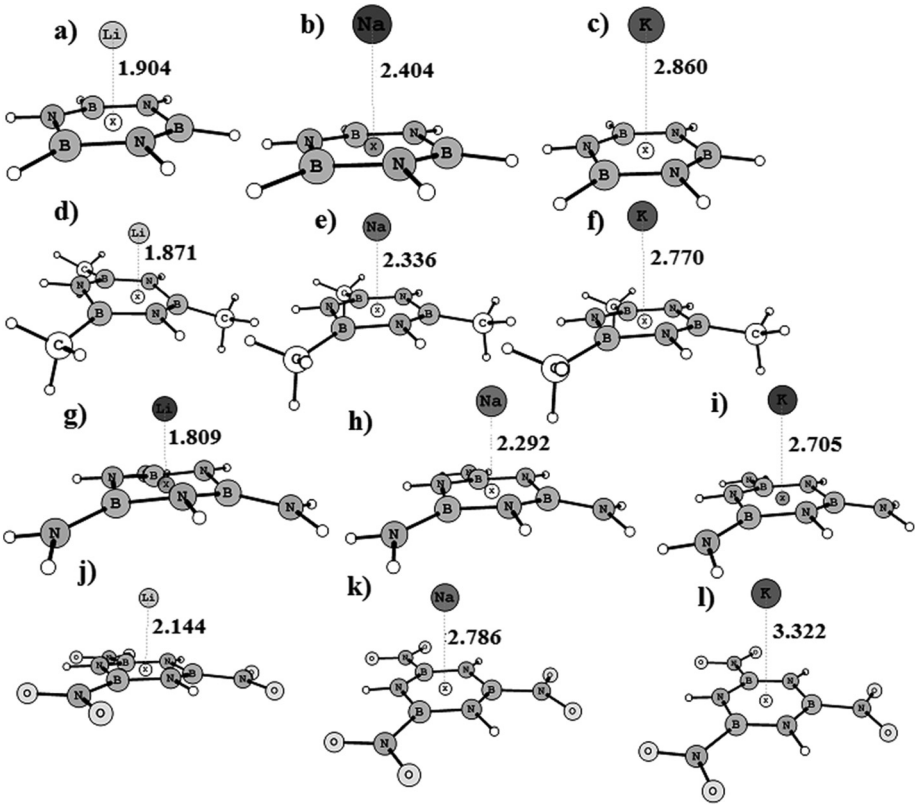

Fig. 2 Optimized geometries at the MP2/6-31+G(d) level of theory of the cation–π complexes of borazine (a–c) and substituted borazines (d–l). Here, X is the geometric mean of the ring the cation–π distances are in angstroms (Å).

Table 1 Geometrical parameters of benzene and borazine and their cationic complexes computed at the MP2/6-31+G(d) level. Bond lengths are in angstroms (Å) and angles are in degrees (°)

Systems	r_{C-C}	r_{X-M}	Systems	r_{B-N}	r_{X-M}	∠NBNB
Benzene	1.399		Borazine	1.435		0.0
Benzene–Li^+	1.407	1.931	Borazine–Li^+	1.448	1.940	18.9
Benzene–Na^+	1.405	2.416	Borazine–Na^+	1.445	2.404	15.3
Benzene–K^+	1.403	2.887	Borazine–K^+	1.442	2.860	14.1
Benzene–$(CH_3)_3$–Li^+	1.411	1.871	Borazine–$(CH_3)_3$–Li^+	1.458	1.833	22.8
Benzene–$(CH_3)_3$–Na^+	1.408	2.369	Borazine–$(CH_3)_3$–Na^+	1.460	2.336	23.6
Benzene–$(CH_3)_3$–K^+	1.406	2.822	Borazine–$(CH_3)_3$–K^+	1.449	2.770	17.9
Benzene–$(NH_2)_3$–Li^+	1.412	1.883	Borazine–$(NH_2)_3$–Li^+	1.466	1.808	30.7
Benzene–$(NH_2)_3$–Na^+	1.408	2.374	Borazine–$(NH_2)_3$–Na^+	1.460	2.292	23.7
Benzene–$(NH_2)_3$–K^+	1.404	2.776	Borazine–$(NH_2)_3$–K^+	1.455	2.704	21.2
			Borazine–$(NO_2)_3$–Li^+	1.430	2.143	16.7
			Borazine–$(NO_2)_3$–Na^+	1.425	2.786	12.2
			Borazine–$(NO_2)_3$–K^+	1.423	3.322	10.8

EDGs and EWGs can be attributed to the involvement of these bonds in the charge transfer transition with the alkali metal cations. Elongation of the bonds advocates the crucial role played by EDGs on charge transfer transitions *i.e.* the transition of electron density of either C–C or B–N bonds to the alkali metal cations, and therefore helping to build up a strong interaction between them.[31,33] In contrast to the above observation regarding EDGs, the presence of EWGs at the 1, 3 and 5 positions of benzene does not lead to the formation of cation–π complexes. This is due to the withdrawal of the σ and π electron density of the B–N bonds by the $–NO_2$ group attached to the B-atoms which thereby hinders the cation–π interactions.

In a similar manner to that of the C–C and B–N bonds of benzene and borazine, respectively, the distance between X and M, denoted as r_{X-M} (where X is the geometric mean of the ring and M is the alkali metal cation) is also influenced by the presence of EDGs and EWGs. $–NH_2$ substituted benzene rings show the shortest r_{X-M} distance and the same is observed in the case of the $–CH_3$ substituted borazine ring, Fig. 1 and 2. An increase in r_{X-M} distance with an increasing size of alkali metal cation indicates that smaller metal cations are greatly

attracted to the π-electron cloud of benzene and borazine. The alkali metal cation–π complexes of benzene are found to be perfectly planar with equal C–C bonds. However, the rings of the cationic complexes of borazine adopt a "puckered structure" (Fig. 2). This loss in planarity, upon complexation with cations, is caused by the synergistic effect resulting from the attraction between the cations and nitrogen atoms and the simultaneous repulsion between the cations and boron atoms. As a result, the three nitrogen atoms are dragged closer to the cation and the boron atoms are pushed away from the plane. This loss of planarity is further reflected in the change in the dihedral angle ∠NBNB in borazine complexes, depicted in Table 1. Additionally, we observed a very good correlation between the ∠NBNB angles and the r_{X-M} distance of the borazine rings. For a particular metal centre in borazine, the larger the dihedral angle ∠NBNB, the shorter the r_{X-M} distance (Fig. 3). This implies that a stronger cation–π interaction is observed for the borazine ring with the greatest loss in planarity. It is noteworthy to mention that, for a particular alkali metal cation, the highest value of dihedral angle is obtained with $-NH_2$ substitutions while the lowest value is obtained for those with $-NO_2$ substituted borazine. This also implies that EDGs like $-NH_2$ lead to a stronger cation–π interaction while EWGs like $-NO_2$ lead to a weaker one. Furthermore, the borazine ring with the greatest loss in planarity (*i.e.*, the highest value of ∠NBNB) has the longest B–N bonds in their cationic complexes (borazine–$(NH_2)_3$–Li^+, Table 1). However, it is surprising to note that despite the loss of planar geometry, we observed that all of the B–N bonds in the cationic complexes were equal. This observation is quite unexpected as complexation with a cation results in a puckered structure of the borazine ring and thus, it is expected that the B–N bond lengths within the complexes should not be equal. In order to authenticate the observed result, we also performed full optimization of the $B_3N_3H_6$–Li^+ complex at different levels of theory (MP2/TZVP and MP2/Aug-ccPVTZ)[34] which demonstrated similar results, Fig. S1.†

Topological analysis

To rationalize the above unexpected observation, we performed topological analysis within the realm of quantum theory of atoms in molecules (QTAIM).[35] The topological parameters of the C–C and B–N bonds within the Li^+ complexes of the parent benzene and borazine are given in Table 2. As expected, the C–C bonds in benzene have a high electron density value at the bond critical point, a higher delocalization index, a greater negative Laplacian value and a higher ellipticity compared to the B–N bonds in borazine. This is due to the polar nature of the B–N bonds in borazine. The value of ellipticity at the B–N bond critical point in a free borazine molecule is very small (0.016) compared to the C–C bonds in benzene indicating that there is a much smaller double bond character and π electron delocalization in the B–N bonds. It should be noted that due

Table 2 Electron density (ρ_b) at the C–C or B–N bond critical points, delocalization index of the C–C and B–N bonds, δ(C,C)/δ(B,N), Laplacian of the electron density at the bond critical point, $\nabla^2\rho$(bcp) and ellipticity (ε) of the C–C and B–N bonds in their Li^+ complexes. All parameters are in a.u.

Systems	ρ_b	δ(C,C)/δ(B,N)	$\nabla^2\rho$(bcp)	ε
Benzene	0.307	1.180	−0.836	0.204
Borazine	0.193	0.440	0.602	0.016
Benzene–Li^+	0.304	1.179	−0.811	0.195
Benzene–$(CH_3)_3$–Li^+	0.309	1.177	−0.813	0.199
Benzene–$(NH_2)_3$–Li^+	0.310	1.178	−0.812	0.197
Borazine–Li^+	0.187	0.435	0.575	0.046
Borazine–$(CH_3)_3$–Li^+	0.189	0.445	0.587	0.049
Borazine–$(NH_2)_3$–Li^+	0.188	0.467	0.579	0.053
Borazine–$(NO_2)_3$–Li^+	0.176	0.423	0.588	0.034

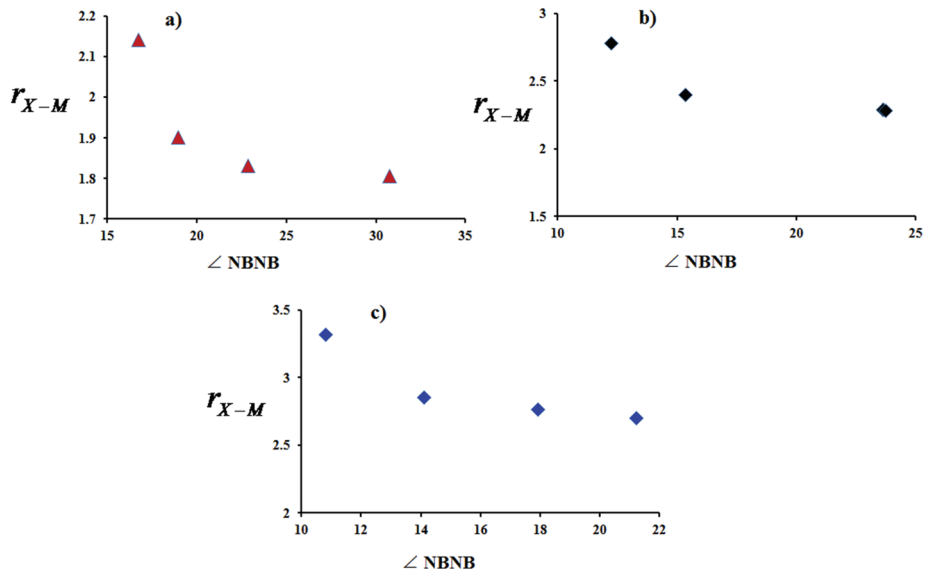

Fig. 3 Correlation between the ∠NBBN dihedral angle (in degrees) and r_{X-M} distance (in Å) for (a) Li^+, (b) Na^+ and (c) K^+ complexes of borazine with different substituents.

to the polar nature of the B–N bonds, a comparison of the π-electron delocalization in benzene and borazine is not justified. However, it may be justifiable to use any changes in the ellipticity of the C–C or B–N bonds within benzene or borazine derivatives alone, to understand the degree of π-electron delocalization. In this regard, we calculated the ellipticity of the C–C and B–N bonds in their Li^+ complexes. It is evident from Table 2 that, complexation of a Li^+ ion with the parent benzene ring slightly decreases the ellipticity of the C–C bonds from 0.204 to 0.195. In contrast, there is an increase in the ellipticity value from 0.016 to 0.053 due to Li^+ complexation with borazine. This implies that complexation of cations increases the π-electron delocalization of the B–N bonds. Thus, despite the non-planar geometry of the borazine ring in the complex, the B–N bonds are found to be equal.

Table 3 contains the QTAIM parameters of the C–M and N–M bond critical points of benzene and borazine respectively. All the benzene–M^+ complexes have six C–M bond critical points indicating that the benzene ring in these complexes has η^6 coordination, Fig. S2.† On the other hand, all the borazine rings within the cationic complexes have an η^3 coordination mode. The nitrogen atoms of the borazine molecule are bonded to the cations *via* electrostatic interactions. The delocalization index of the C–M and N–M bonds for a particular metal centre increases as the aromatic rings are substituted with $-CH_3$ and $-NH_2$. In contrast, delocalization decreases dramatically for $-NO_2$ substituted borazine rings. The values of Laplacian $\nabla^2\rho$(bcp) and total electronic energy density $H(r)$, are positive and close to zero indicating the electrostatic nature of the C–M and N–M bonds. The ratio of the kinetic energy density to that of the electron density, G_b/ρ_b, at the C–M and N–M bonds in these complexes is greater than zero for all the metals except K^+, supporting the electrostatic interaction between them. Charge transfer from the parent benzene ring to the cation is lower than that from the parent borazine ring. However, substituents such as $-CH_3$ and $-NH_2$ attached to the benzene ring increases the charge transfer. This might be due to the electron pushing ability of these substituents resulting in a greater charge transfer from the benzene ring to the cation. The highest value of charge transfer is found with $-NH_2$ substituted rings while the lowest is found for the $-NO_2$ substituted borazine.

Binding energy

In order to investigate the strength of the interaction between the metal cation and the ring π-cloud, we have calculated the binding energy of the complexes. The gas phase binding energy (ΔE) values of the cation–π complexes are obtained from both DFT and MP2 calculations. The basis set superposition error (BSSE) corrected binding energy values are given in Table 4. A greater negative value of binding energy indicates the formation of a more stable cation–π complex. These binding energy (ΔE) values are almost comparable to those reported for the cation–π complexes of benzene and borazine.[26,31,36] The binding energy values are found to be strongly dependent on the size of the cation and the nature of the substituents. At all levels of calculation, both benzene and borazine cation–π complexes show the same order of binding energy *i.e.* $Li^+ > Na^+ > K^+$. A similar trend in binding energy values was obtained by Dougherty for cation–π complexes of

Table 3 QTAIM parameters at the bond critical points of the C–M and N–M bonds of benzene and borazine respectively. All parameters are in a.u.

$C_6H_3(R)_3$–M^+							
R	M	ρ_b	δ(C,M)	$\nabla^2\rho$(bcp)	$H(r)$	G_b/ρ_b	$q\lvert C \rightarrow M\rvert$
H	Li	0.014	0.026	0.073	0.003	1.108	0.131
	Na	0.010	0.027	0.047	0.002	1.010	0.133
	K	0.008	0.032	0.023	0.001	0.754	0.147
NH_2	Li	0.016	0.034	0.084	0.002	1.062	0.292
	Na	0.011	0.031	0.054	0.002	1.004	0.278
	K	0.011	0.039	0.042	0.001	0.731	0.301
CH_3	Li	0.015	0.031	0.084	0.003	1.133	0.278
	Na	0.011	0.030	0.053	0.002	1.002	0.282
	K	0.009	0.038	0.036	0.001	0.728	0.328
$H_3B_3N_3(R)_3$–M^+							
R	M	ρ_b	δ(N,M)	$\nabla^2\rho$(bcp)	$H(r)$	G_b/ρ_b	$q\lvert N \rightarrow M\rvert$
H	Li	0.014	0.043	0.081	0.003	1.190	0.280
	Na	0.010	0.043	0.049	0.002	1.000	0.283
	K	0.009	0.054	0.034	0.001	0.780	0.285
NH_2	Li	0.018	0.052	0.107	0.004	1.220	0.288
	Na	0.013	0.052	0.066	0.002	1.070	0.290
	K	0.012	0.068	0.047	0.002	0.830	0.292
CH_3	Li	0.017	0.049	0.097	0.004	1.176	0.285
	Na	0.012	0.049	0.058	0.003	1.082	0.290
	K	0.010	0.064	0.040	0.002	0.800	0.292
NO_2	Li	0.012	0.012	0.078	0.003	1.187	0.121
	Na	0.009	0.014	0.067	0.002	1.163	0.124
	K	0.009	0.018	0.051	0.002	0.840	0.127

Table 4 Counterpoise corrected interaction energies (in kcal mol^{-1}) in the B3LYP and MP2 methods

	B3LYP			MP2		
Systems	6-31+G(d)	6-31++G(d,p)	6-311++G(d,p)	6-31+G(d)	6-31++G(d,p)	6-311++G(d,p)
Benzene–Li^+	−36.84	−36.71	−37.79	−34.13	−33.14	−34.70
Benzene–Na^+	−23.78	−23.64	−23.19	−21.77	−21.02	−20.71
Benzene–K^+	−15.14	−15.02	−15.88	−15.74	−15.20	−16.96
Benzene–$(CH_3)_3$–Li^+	−44.45	−44.45	−46.00	−43.65	−41.51	−43.42
Benzene–$(CH_3)_3$–Na^+	−28.66	−28.70	−28.59	−26.18	−25.44	−25.52
Benzene–$(CH_3)_3$–K^+	−12.51	−12.76	−14.40	−13.49	−13.88	−15.46
Benzene–$(NH_2)_3$–Li^+	−55.34	−55.42	−56.43	−50.13	−49.55	−51.25
Benzene–$(NH_2)_3$–Na^+	−39.36	−39.27	−38.83	−35.46	−34.96	−34.69
Benzene–$(NH_2)_3$–K^+	−29.17	−28.98	−30.18	−29.06	−28.65	−30.79
Borazine–Li^+	−30.26	−30.02	−31.27	−29.54	−28.63	−29.69
Borazine–Na^+	−18.87	−18.63	−18.73	−18.26	−17.57	−17.38
Borazine–K^+	−11.51	−11.23	−11.90	−12.82	−12.29	−13.39
Borazine–$(CH_3)_3$–Li^+	−39.89	−39.78	−40.98	−38.53	−37.37	−38.42
Borazine–$(CH_3)_3$–Na^+	−25.53	−25.36	−25.43	−24.48	−23.58	−23.36
Borazine–$(CH_3)_3$–K^+	−15.69	−15.50	−16.48	−17.52	−16.90	−18.37
Borazine–$(NH_2)_3$–Li^+	−52.98	−52.52	−53.67	−52.27	−51.00	−51.93
Borazine–$(NH_2)_3$–Na^+	−37.47	−36.99	−37.00	−36.82	−35.83	−35.61
Borazine–$(NH_2)_3$–K^+	−26.97	−26.43	−27.37	−28.87	−28.10	−29.74
Borazine–$(NO_2)_3$–Li^+	7.31	7.51	7.12	7.35	6.05	5.18
Borazine–$(NO_2)_3$–Na^+	13.06	13.27	14.81	9.02	7.63	9.97
Borazine–$(NO_2)_3$–K^+	13.77	13.92	15.19	8.91	7.39	9.15

benzene in a gas phase.[37] On substituting with the EDGs, the interaction energy is found to be enhanced. In both benzene and borazine, the –NH_2 substituted Li^+–cation–π complexes show the maximum binding energy (>−50 kcal mol^{-1}). Among all the cation–π complexes, benzene–$(NH_2)_3$–Li^+ gives the highest ΔE of −55.34 kcal mol^{-1} at the B3LYP/6-31+G(d) level of calculation. Surprisingly, upon substituting with EWGs, the binding energy values decrease. The lowest binding energy value is found in the case of the borazine–$(NO_2)_3$–K^+ complex (13.77 kcal mol^{-1} at the B3LYP/6-31+G(d) level). This indicates that both the size of the cation and the nature of the substituents influence the cation–π interaction energy. The increase in the basis set size does not affect the ΔE values to a larger extent, Table 4. Thus, the B3LYP/6-31+G(d) energy value for Li^+ differs only by 0.13 kcal mol^{-1} and −0.5 kcal mol^{-1} from those obtained by B3LYP/6-31++G(d,p) and B3LYP/6-311++G(d,p), respectively. Similar to the B3LYP calculations, the MP2 binding energy values presented in Table 4 do not show much more deviation even with the increase in basis set size. Furthermore, the B3LYP values differ only by 2 to 5 kcal mol^{-1} from those of the MP2. These results are consistent with previously reported values.[33,36] The BSSE corrections are less at the B3LYP level than with the MP2 calculation (see Table S1 ESI†). The BSSE corrections at the B3LYP/6-31G(d) level range from 0.29 to 1.02 kcal mol^{-1}. The MP2, ΔE_{BSSE} values are more significant, varying from 1.56 to 4.68 kcal mol^{-1}. Thus, BSSE corrections can be as large as 15% of the raw binding energies at the MP2/6-31+G(d) level of theory, Table 5.

The strength of the bonds between the ring and the metal centre has been assessed by force constants (Table 5). It is evident from Table 5 that, the force constants of the bonds are higher for the substituted rings compared with the parent ring. The calculated binding energy of the cations to the six

Table 5 The gas phase calculated raw binding energy (in kcal mol^{-1}) at the MP2/6-31+G(d) level of theory and force constant (10^{-3} × Dyne Å^{-1}) of the bonds between the ring and the metal centre

	M = Li^+		Na^+		K^+	
Systems	ΔE	k	ΔE	k	ΔE	k
Benzene	−38.7	0.51	−25.6	0.31	−18.1	0.15
Benzene–$(CH_3)_3$	−45.8	0.52	−30.4	0.38	−24.0	0.17
Benzene–$(NH_2)_3$	−55.0	0.55	−39.8	0.41	−34.0	0.18
Borazine	−32.8	0.47	−21.3	0.31	−15.7	0.16
Borazine–$(CH_3)_3$	−42.1	0.54	−28.1	0.36	−21.7	0.19
Borazine–$(NH_2)_3$	−56.0	0.55	−40.7	0.46	−33.5	0.28
Borazine–$(NO_2)_3$	2.24	0.16	6.88	0.12	5.98	0.09

membered rings increases for –CH_3 and –NH_2 substituted rings. –NO_2 substituted borazine shows a positive value of binding energy, denying the formation of stable complexes. A nice correlation has been obtained between the binding energy and the force constant as well as the charge transfer values. A complex with a higher binding energy possesses a higher value of the force constant and a higher value of charge transfer from the ring to the metal centre. This indicates that the electrostatic interaction and the charge transfer transition contributes to the total binding energy of the complexes. Similar to our results, Jiang and co-workers through their KM (Kitaura–Morokuma) and RVS (Reduced Variational Space) energy decomposition analysis, have shown that the cation–π interaction is driven by electrostatic charge transfer and polarization terms and contributes to the overall binding energies.[38] Kim and co-workers,[39] Sherill and co-workers[40] and several other prominent studies using a SAPT (Symmetry Adapted Perturbation Theory) method, have reported that both electrostatic and induction effects contribute to the cation–π interaction energies of different types of cations (*viz.* Li^+, Na^+,

K^+, Mg^{2+}, Ca^{2+}, Ag^+, NH_4^+, $C(NH_2)_3^+$, $N(CH_3)_4^+$), with various organic aromatic π-systems (ethene, benzene and pyrrole).[41] Studies made by Hanusa and coworkers[42] using the ADF (Amsterdam Density Functional) program on the energetics suggests that the basis for the origin of the differences in the binding of metal cations to two ethylene molecules as against benzene is a consequence of the larger contribution from the polarization/charge transfer term for two ethylenes compared to benzene.

Effect of solvent and substituent on binding energy

Cation–π interaction energies are highly influenced by the nature of the solvent. Dougherty found that the order of cation–π interaction energy in the gas phase was $Li^+ > Na^+ > K^+ > Rb^+$ whereas, in an aqueous phase the order was $K^+ > Rb^+ \gg Na^+$, Li^+.[37] Thus, to understand the effect of solvents on the cation–π interaction energy in benzene and borazine, we choose three different solvent systems *viz.* benzene, acetone and water; results are summarised in Table 6. In the gas phase, irrespective of any substituent(s), in both benzene and borazine cation–π complexes, we observed the same trend as observed by Dougherty.[37] Similarly, in the presence of acetone and water as the solvent, we observed the same order *i.e.* $K^+ > Na^+ > Li^+$. And, where the substituent effect is concerned, it is the $–NH_2$ group which highly favours the cation–π interaction in both benzene and borazine. Table 6 shows that the strength of the cation–π interaction gets substantially reduced in the presence of polar solvents. Changes in the cation–π interaction energy, with respect to the solvent polarity, can be attributed to the fact that Li^+ ions bind strongly to π systems, but at the same time, they are highly solvated in aqueous solution. Therefore, the desolvation energy is too high for them to bind to the benzene ring. Compared with Li^+, K^+ ions are less strongly solvated by water but are still good π binders. As a result, K^+ ions bind with the benzene and borazine ring even in aqueous solution. Interestingly, when benzene is employed as a solvent, the order of the cation–π interaction energy in unsubstituted benzene is $Li^+ > K^+ > Na^+$, whereas in borazine it is $K^+ > Li^+ > Na^+$. However, in the case of $–CH_3$ and $–NH_2$ substitutions, both benzene and borazine show the same order *i.e.* $Li^+ > K^+ > Na^+$.

The effect of water molecules on solvating the metal ion in the cation–π interaction, has been reported by various groups.[43] Recently, Rao *et al.*[36] have investigated the effect of solvation on the interaction energy of various cation–π complexes of benzene *via* a discrete solvation model. However, to the best of our knowledge, such studies have not been implemented in the case of borazine. Therefore, in order to investigate such an effect in our study, we consider only borazine and its substituted derivatives. A few hydrated borazine–Li^+ complexes are depicted in Fig. 4 as representatives (all other structures of the complex are provided in the ESI, Fig. S3–S5†). From Fig. 4, it is clear that when water molecules are present either in the plane or below the plane of borazine, the cation–π distance is shorter compared to that in the bare cation–π system (Fig. 2). For example, the cation–π distance in Li^+–π–W (W = water) is 1.935 Å; this is 0.050 Å shorter than the cation–π distance (1.940 Å) in the bare (without solvent) Li^+–π complex. This result is consistent with those obtained with the Li^+–π complex of benzene.[36] However, in the case of Na^+–π–W and K^+–π–W, the cation–π distance is found to increase by 0.028 Å and 0.187 Å, respectively. In the case of $–CH_3$ and $–NH_2$ substituted borazine, the M–π (M = Li^+, Na^+, K^+) distance decreases further compared to the parent complex and this significant decrease is found with Li^+–π complexes, Table 7. This indicates that when the metal ions are solvated, electron donating groups favour the cation–π interaction. Furthermore, increasing the number of water molecules near the borazine further shortens the cation–π distance. The shortest cation–π distance (1.838 Å) is seen in the case of the Li^+–π–5W complex, which contains five water molecules; out of these, three are connected to borazine protons through N–H···O hydrogen bonding and the other two are above and below the plane of the borazine ring (see Fig. 4). This is in agreement with earlier studies which showed that solvated benzene cation–π complexes have C–H···O type hydrogen bonding.[36]

The interaction energies calculated by B3LYP/6-31++G(d,p) for the solvated complexes are compiled in Table 7. Rao *et al.*[36]

Table 6 Cation–π interaction energy (in kcal mol^{-1}) of benzene, borazine and their substituted derivatives in different solvent medium at the MP2/6-31+G(d) level of calculation

	Interaction energy, Δ*E*				Interaction energy, Δ*E*		
Systems	Benzene	Acetone	Water	Systems	Benzene	Acetone	Water
Benzene–Li^+	−9.5	6.6	7.8	Borazine–Li^+	−3.9	12.1	13.2
Benzene–Na^+	−7.3	2.2	2.8	Borazine–Na^+	−3.5	5.5	6.1
Benzene–K^+	−7.4	−1.6	−1.2	Borazine–K^+	−5.1	0.4	0.8
Benzene–$(CH_3)_3$–Li^+	−12.7	5.8	7.1	Borazine–$(CH_3)_3$–Li^+	−9.0	9.8	11.2
Benzene–$(CH_3)_3$–Na^+	−9.3	1.5	2.2	Borazine–$(CH_3)_3$–Na^+	−7.2	3.9	4.6
Benzene–$(CH_3)_3$–K^+	−10.7	−3.9	−3.5	Borazine–$(CH_3)_3$–K^+	−8.6	−1.5	−1.0
Benzene–$(NH_2)_3$–Li^+	−19.2	4.1	6.2	Borazine–$(NH_2)_3$–Li^+	−18.6	5.8	7.9
Benzene–$(NH_2)_3$–Na^+	−16.0	0.05	1.5	Borazine–$(NH_2)_3$–Na^+	−15.6	0.9	2.4
Benzene–$(NH_2)_3$–K^+	−17.6	−5.5	−4.3	Borazine–$(NH_2)_3$–K^+	−16.4	−4.0	−3.0
				Borazine–$(NO_2)_3$–Li^+	26.4	28.0	27.4
				Borazine–$(NO_2)_3$–Na^+	19.1	15.2	14.2
				Borazine–$(NO_2)_3$–K^+	14.9	18.5	9.6

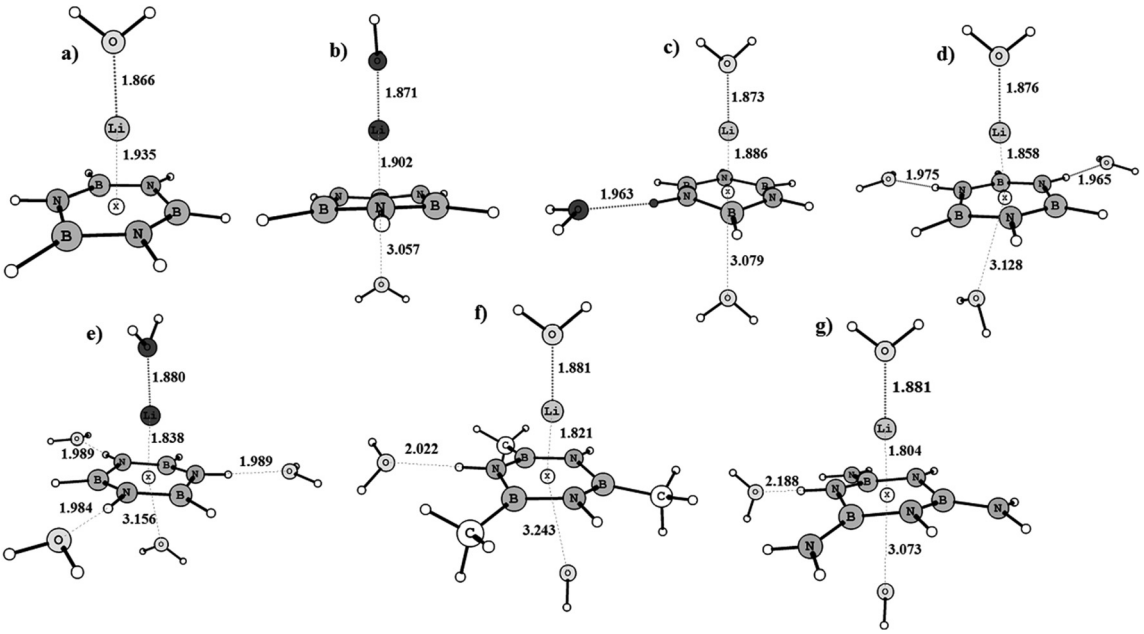

Fig. 4 Optimized geometry at the B3LYP/6-31++G (d,p) level of calculation of (a) borazine–Li^+–π–W, (b) borazine–Li^+–π–2W, (c) borazine–Li^+–π–3W, (d) borazine–Li^+–π–4W, (e) borazine–Li^+–π–5W, (f) borazine $(CH_3)_3$–Li^+–π–3W, (g) borazine $(NH_2)_3$–Li^+–π–3W. The distances shown by the dotted lines are in angstroms (Å).

Table 7 Counterpoised corrected interaction energies (in kcal mol^{-1}) at the B3LYP/6-31++G(d,p) level of calculation, M–π distances (M = Li^+, Na^+, K^+) and N–H···O distances (in Å) in water solvated cation–π complexes of borazine. W represents the number of water molecules

Systems	ΔE_{int}	ΔE_{BSSE}	M–π distance (Å)	N–H···O (Å)
Borazine–Li^+–π–W	−58.53	1.72	1.935	
Borazine–Na^+–π–W	−40.20	1.67	2.432	
Borazine–K^+–π–W	−27.27	0.91	2.993	
Borazine–Li^+–π–2W	−64.12	2.75	1.902	
Borazine–Na^+–π–2W	−44.80	2.82	2.390	
Borazine–K^+–π–2W	−30.99	1.76	2.934	
Borazine–Li^+–π–3W	−72.71	3.65	1.886	1.963
Borazine–Na^+–π–3W	−52.76	3.68	2.362	1.974
Borazine–K^+–π–3W	−38.38	2.56	2.900	2.004
Borazine–Li^+–π–4W	−80.64	4.48	1.858	1.965, 1.975
Borazine–Na^+–π–4W	−59.99	4.62	2.343	1.991, 2.001
Borazine–K^+–π–4W	−45.08	3.38	2.873	2.032, 2.017
Borazine–Li^+–π–5W	−87.84	5.31	1.838	1.989, 1.989, 1.984
Borazine–Na^+–π–5W	−66.66	5.50	2.323	2.015, 2.007, 2.015
Borazine–K^+–π–5W	−51.26	4.17	2.840	2.031, 2.050, 2.043
Borazine–$(CH_3)_3$–Li^+–W	−66.18	1.91	1.862	
Borazine–$(CH_3)_3$–Na^+–W	−45.85	1.90	2.351	
Borazine–$(CH_3)_3$–K^+–W	−31.25	1.15	2.900	
Borazine–$(CH_3)_3$–Li^+–2W	−70.76	2.81	1.841	
Borazine–$(CH_3)_3$–Na^+–2W	−49.63	3.03	2.328	
Borazine–$(CH_3)_3$–K^+–2W	−34.50	1.97	2.866	
Borazine–$(CH_3)_3$–Li^+–3W	−78.11	3.69	1.821	2.022
Borazine–$(CH_3)_3$–Na^+–3W	−56.24	4.04	2.319	2.063
Borazine–$(CH_3)_3$–K^+–3W	−40.82	2.77	2.846	2.070
Borazine–$(NH_2)_3$–Li^+–W	−77.07	2.03	1.837	
Borazine–$(NH_2)_3$–Na^+–W	−56.17	2.03	2.301	
Borazine–$(NH_2)_3$–K^+–W	−40.72	1.18	2.815	
Borazine–$(NH_2)_3$–Li^+–2W	−80.37	2.94	1.823	
Borazine–$(NH_2)_3$–Na^+–2W	−58.74	3.26	2.322	
Borazine–$(NH_2)_3$–K^+–2W	−44.76	1.99	2.790	
Borazine–$(NH_2)_3$–Li^+–3W	−88.53	3.99	1.840	2.188

reported that in the case of benzene cation–π complexes, the strength of the cation–π interaction depends on the site of solvation. It was reported that solvation of the metal ion decreases its interaction energy with the π system, while the solvation of the π system increases its interaction energy with the metal ion. However, our model on borazine suggests that

interaction energy values increase continuously upon increasing the number of water molecules and is further enhanced by an EDG. It is found to be −58.53 kcal mol^{-1} in the case of borazine–Li$^+$–π–W and −87.84 kcal mol^{-1} in the case of borazine–Li$^+$–π–5W. On the other hand, borazine–$(CH_3)_3$–Li$^+$–3W has an interaction energy of −78.11 kcal mol^{-1} and borazine–$(NH_2)_3$–Li$^+$–3W has an interaction energy of −88.53 kcal mol^{-1}. This implies that EDGs greatly influence the interaction energy of solvated cation–π complexes. Thus, the presence of the metal ion polarizes the B–N bond in borazine and facilitates its interaction with the solvent molecules through N–H···O hydrogen bonding and thereby strengthens the cation–π interaction energy in comparison to those of benzene.[36] The interaction energy values show good correlation (R^2 > 0.82, Fig. S6†) with M–π distances indicating that the cation–π interaction energy is highly influenced by M–π distances. Comparisons of the cation–π interaction energy of the discrete solvation model[36] with those of the PCM-model at the same level of theory (Table S2†) highlights differences in the order. However, the trend is consistent with those in the gas phase. This is expected because in the polarized continuum model (PCM), solvents are modeled as a polarizable continuum, and not as individual molecules.

Correlation between Hammett constant and aromaticity with binding energy

Non-covalent interactions of aromatics with other aromatics, with cations, and with anions are understood in terms of the Hammett substituent constants.[44,45] Out of these three general types of aromatic non-covalent interactions, studies of arene–arene interactions were the first to employ Hammett constants as a means of understanding the binding.[46] However, there are very few reports investigating the correlation between cation–π binding energies and Hammett substituent constants compared with arene–arene interactions.[47] Dougherty and co-workers appear to be the first researchers to suggest a possible relationship between cation–π binding and Hammett substituent constants.[48] Jiang and co-workers also found excellent correlation between the binding enthalpies and the total Hammett parameter, σ_{Total}.[49] Therefore, in order to obtain the correlation between the interaction energy and Hammett constants, we performed a linear regressional analysis. Fig. 5, Fig. S7 and S8 (see ESI†) show the plot of interaction energy (at the MP2/6-31+G(d) level of theory) as a function of the Hammett constants, σ_m, σ_p and the total Hammett parameter defined as $\sigma_{Total} = (\sum\sigma_m + \sum\sigma_p)$, respectively. σ_m constants provide a measure of the inductive electron-withdrawal or donation by the substituent (inductive effect). The σ_p Hammett constant describes the movement of electrons *via* the σ- and π-framework (inductive and resonance effects). We have obtained a very good correlation between the interaction energy (ΔE) and σ_m, σ_p and $\sigma_{Total} = (\sum\sigma_m + \sum\sigma_p)$ indicating that the trend in the substituent effects can be qualitatively understood in terms of the electron-donating or withdrawing characteristic of the substituents. The borazine–K$^+$ complexes in the presence of benzene as a solvent show a very poor relationship (obtained using PCM model). The absence of a correlation also clearly explains the anomalous trends in binding energies shown by these complexes in the presence of benzene as a solvent (see Table 6, PCM model). However, in all other complexes excellent correlation (R^2 > 9, Table S3†) is observed in both gas and solvent phases (water and acetone), indicating that the cation–π binding is dependent on the nature of the substituents. Furthermore, correlation with σ_m,

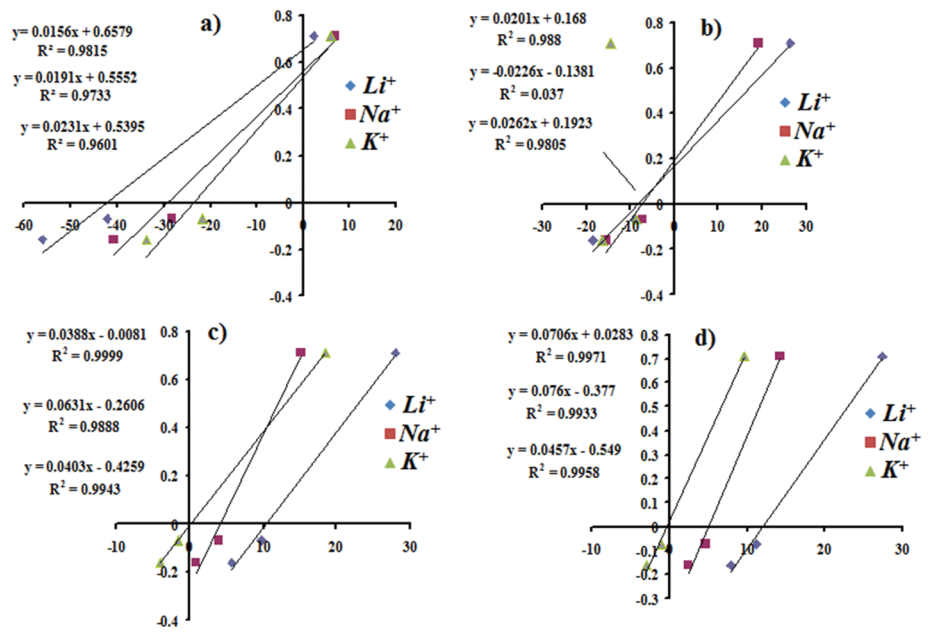

Fig. 5 Correlation plot between the interaction energies (*X*-axis) of various substituted cation–π complexes of borazine and the Hammett constant (σ_m, *Y*-axis) (a) in the gas phase, (b) in benzene medium, (c) in acetone medium and (d) in water medium.

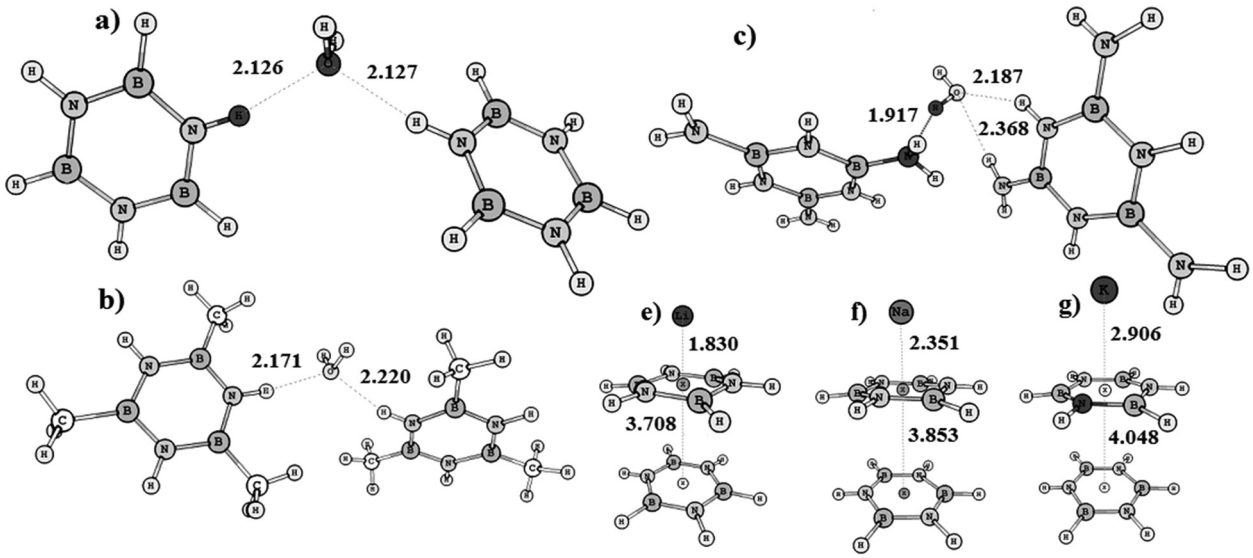

Fig. 6 Optimized geometries at B3LYP/6-31++G(d,p) of benzene and $-CH_3$ and $-NH_2$ substituted derivatives showing H-bonding cooperativity (a–c) and π–π stacking in borazine in the presence of an alkali metal cation (e–g). The distances shown by the dotted lines are in angstroms (Å).

σ_p and $\sigma_{Total} = (\sum\sigma_m + \sum\sigma_p)$ signifies that both resonance and induction are important for cation–π binding in borazine.

The effects of the cation–π interaction on the aromaticity of these six membered rings are further assessed by nucleus independent chemical shift (NICS) calculations at the B3LYP/6-31+G(d) level. The calculated NICS values at the geometrical mean of the ring, NICS(0), and at 1 Å above the ring, NICS(1), reveal that the binding of the cations (Li^+, Na^+, K^+) to benzene and the substituted benzene rings, do not affect the ring currents significantly, although a marginal decrease in the ring currents is observed (see Table S4, ESI†). Moreover, we do not find any correlation between the NICS values and binding energies. We could not calculate the NICS values for the cationic complexes of borazine and substituted borazine due to the puckered geometry of the complexes. Several other groups have also reported that the NICS values obtained at or above the ring center do not parallel other structural, magnetic or energetic criteria,[50–52] or even contrast with experimentally observed molecular behaviours in some cases, other than hydrocarbon aromatic molecules.[53]

Effect of cation–π interaction in cooperative induction (H-bonding and π–π stacking)

Cooperativity is a well studied phenomenon in biology and hydrogen bonded clusters.[31] In contrast, there are much fewer studies estimating cooperativity in systems involving the cation–π interaction.[54,55] G. N. Sastry and his co-workers[54] found that complexation of phenol with Li^+ or Mg^{2+} in either a π- or σ-fashion strengthens the phenol–H_2O hydrogen bonding interaction energy by about 2 and 7 kcal mol^{-1} in Li^+ and Mg^{2+} complexes, respectively. It was also observed that there was a notable enhancement in the π–π stacking of the benzene ring in the presence of cations.[55] In order to investigate the role of the cation–π interaction in co-operative induction, we considered borazine in a similar study.

The optimized geometries showing the H-bonding cooperativity and π–π stacking for borazine and its substituted derivatives are given in Fig. 6. While observing the role of the cation–π interaction in H-bonding cooperativity, we found that in the absence of any cation, borazine and two of its substituted derivatives showed H-bonding cooperativity through water *via* N–H···O interaction. The N–H···O bond length ranged from 1.917 to 2.220 Å which is in agreement with the literature value.[56] However, in the presence of cations such cooperativity is strongly opposed. This implies that in the case of borazine, the cation–π interactions disrupt the H-bonding cooperativity whereas in the case of phenol, it has been found to be enhanced.[54] Interestingly, we observed unfavourable face to face π–π stacking between two borazines. However, in the presence of cations, similar to the case of benzene, the face to face π–π stacking between two borazines is found to be more feasible and is greatly favoured in the case of Li^+. The distance between the two rings varies from 3.708 Å to 4.048 Å as the size of the cation increases from Li^+ to K^+. This suggests that although cation–π interaction plays a negative role in H-bonding co-operativity, it significantly enhances the π–π stacking in borazine, Scheme 2. The interaction energy values for these systems, predicted in Table S5†, further indicates that binary complexes of borazine exist *via* H-bond interactions (in the absence of cation) and π–π stacking (in the presence of cations).

Reactivity of cation–π complexes

Recently, research based on the weak force of these non-covalent interactions has been well recognized in asymmetric and organo-catalysed reactions.[20] Therefore, as well as knowing the structural and interaction energy of the cation–π complexes, it is equally important to understand the reactivity of such systems. In order to do so, we used global hardness

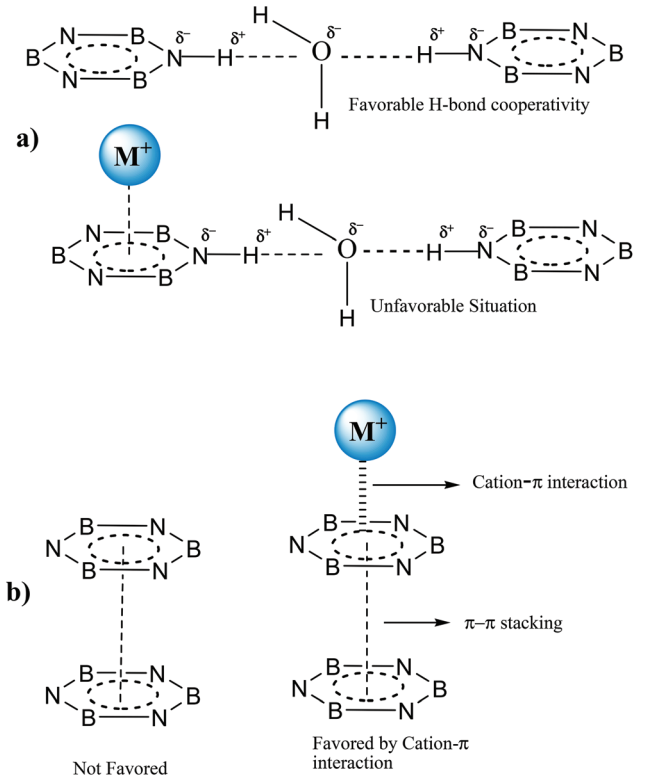

Scheme 2 Schematic representation showing the effect of the cation–π interaction on (a) H-bonding cooperativity and (b) π–π stacking in borazine. The H-atoms of borazine are omitted for clarity.

(η), chemical potential (μ) and electrophilicity index (ω) values to predict the reactivity of such a system.

The gas and solvent phase values of global hardness (η), chemical potential (μ) and electrophilicity index (ω) for benzene and borazine cation–π complexes calculated at the B3LYP/6-31+G(d) level of theory are presented in Tables 8 and 9, respectively. In both the gas and solvent phase, η of the Li^+–cation–π complexes of benzene and borazine is higher than bare benzene and borazine. However, with an increase in the cation size, the η value decreases. According to the maximum hardness principle (MHP),[57] species with the maximum η-value are more stable and least reactive. So, following the MHP, it can be said that the Li^+–cation–π complexes of benzene and borazine are more stable and less reactive in comparison to benzene and borazine. Whereas, the cation–π complexes of Na^+ and K^+ are less stable and more reactive than the parent benzene and borazine. Therefore, by interaction of either benzene or borazine with larger size cations the reactivity of the species can be enhanced. There are recent examples where the cation–π interaction is found to enhance the catalytic activity.[58] The maximum η-value associated with Li^+–π-systems is in accordance with our interaction energy value. Furthermore, on substituting electron-donating groups (EDGs) and electron withdrawing groups (EWGs) on the parent compounds, the η value of the cationic complexes further diminishes. This decrease in the η value becomes more prominent in $-NH_2$ substituted benzene or borazine. Comparisons of the reactivity of benzene and borazine suggest that cation–π complexes of benzene are more reactive compared to borazine. The presence of the electron withdrawing group ($-NO_2$), in the case of borazine, decreases the chemical hardness to a greater extent. This further suggests that borazine–cation–π complexes become more reactive after substitution with an $-NO_2$ group. Furthermore, it can be observed that in the gas phase and in the presence of benzene as a solvent, Li–cation–π complexes of benzene and borazine have the maximum value of η and μ and the minimum value of ω, therefore these complexes will be the least reactive.[59] Whereas, the Na^+–cation–π complexes have the minimum value of η and μ and the maximum value of ω and are more reactive. Among the benzene cation–π complexes, the benzene–$(NH_2)_3$–Na^+ complex with the minimum value of η and μ and the maximum value of ω is the most reactive whereas in the case of borazine, borazine–$(NO_2)_3$–Na^+ is the most reactive. However, on increasing the solvent polarity, the reactivity orders changes. In the presence of water and acetone as the solvent, the cation–π complexes associated with a K^+ ion are found to be the most reactive with a minimum value of η and μ and a maximum value of ω. Thus, it can be concluded that the chemical reactivity of benzene and borazine is

Table 8 Chemical hardness (η in a.u.), chemical potential (μ in a.u.) and electrophilicity index (ω in a.u.) of benzene and its substituted derivatives calculated at B3LYP/6-31+G(d) in the gas phase and in different solvent phases

	In gas phase			Benzene			Acetone			Water		
Systems	η	μ	ω	η	μ	ω	η	μ	ω	η	μ	ω
1. Benzene	0.121	−0.135	0.075	0.121	−0.136	0.076	0.121	−0.138	0.079	0.121	−0.139	0.079
2. Benzene–Li^+	0.336	−0.125	0.023	0.125	−0.225	0.236	0.124	−0.178	0.128	0.124	−0.172	0.120
3. Benzene–Na^+	0.114	−0.320	0.445	0.121	−0.243	0.207	0.122	−0.159	0.112	0.122	−0.155	0.105
4. Benzene–K^+	0.114	−0.299	0.390	0.122	−0.213	0.187	0.121	−0.166	0.104	0.121	−0.160	0.098
5. Benzene–$(CH_3)_3$	0.114	−0.121	0.064	0.114	−0.123	0.066	0.114	−0.125	0.069	0.114	−0.126	0.069
6. Benzene–$(CH_3)_3$–Li^+	0.118	−0.305	0.395	0.117	−0.222	0.211	0.117	−0.163	0.113	0.117	−0.157	0.105
7. Benzene–$(CH_3)_3$–Na^+	0.102	−0.299	0.435	0.111	−0.208	0.188	0.116	−0.145	0.091	0.116	−0.140	0.085
8. Benzene–$(CH_3)_3$–K^+	0.101	−0.284	0.398	0.115	−0.200	0.180	0.115	−0.152	0.100	0.115	−0.147	0.094
9. Benzene–$(NH_2)_3$	0.095	−0.098	0.054	0.097	−0.099	0.050	0.100	−0.101	0.051	0.100	−0.102	0.051
10. Benzene–$(NH_2)_3$–Li^+	0.100	−0.264	0.348	0.105	−0.177	0.152	0.104	−0.125	0.075	0.103	−0.121	0.070
11. Benzene–$(NH_2)_3$–Na^+	0.084	−0.264	0.415	0.094	−0.179	0.166	0.099	−0.122	0.075	0.098	−0.117	0.070
12. Benzene–$(NH_2)_3$–K^+	0.086	−0.249	0.359	0.094	−0.171	0.155	0.097	−0.120	0.074	0.097	−0.116	0.069

Table 9 Chemical hardness (η in a.u.), chemical potential (μ in a.u.) and electrophilicity index (ω) of borazine and its substituted derivatives calculated at B3LYP/6-31+G(d) in the gas phase and in different solvent phases

	In gas phase			Benzene			Acetone			Water		
Systems	η	μ	ω	η	μ	ω	η	μ	ω	η	μ	ω
1. Borazine	0.143	−0.143	0.071	0.143	−0.143	0.071	0.144	−0.142	0.070	0.142	−0.144	0.073
2. Borazine–Li^+	0.147	−0.340	0.393	0.147	−0.245	0.204	0.147	−0.180	0.110	0.147	−0.174	0.102
3. Borazine–Na^+	0.127	−0.335	0.441	0.127	−0.235	0.217	0.145	−0.164	0.092	0.145	−0.159	0.087
4. Borazine–K^+	0.127	−0.314	0.388	0.127	−0.225	0.199	0.143	−0.168	0.098	0.143	−0.164	0.094
5. Borazine–$(CH_3)_3$	0.127	−0.142	0.079	0.127	−0.142	0.079	0.129	−0.142	0.078	0.129	−0.142	0.078
6. Borazine–$(CH_3)_3$–Li^+	0.138	−0.316	0.361	0.138	−0.229	0.190	0.143	−0.168	0.098	0.142	−0.163	0.093
7. Borazine–$(CH_3)_3$–Na^+	0.120	−0.319	0.424	0.120	−0.225	0.210	0.135	−0.159	0.093	0.135	−0.155	0.088
8. Borazine–$(CH_3)_3$–K^+	0.122	−0.299	0.366	0.122	−0.216	0.191	0.133	−0.163	0.099	0.133	−0.157	0.092
9. Borazine–$(NH_2)_3$	0.102	−0.267	0.349	0.102	−0.121	0.071	0.109	−0.124	0.070	0.110	−0.125	0.071
10. Borazine–$(NH_2)_3$–Li^+	0.115	−0.280	0.340	0.115	−0.199	0.172	0.120	−0.147	0.090	0.120	−0.137	0.078
11. Borazine–$(NH_2)_3$–Na^+	0.101	−0.281	0.390	0.101	−0.197	0.192	0.115	−0.141	0.086	0.115	−0.137	0.081
12. Borazine–$(NH_2)_3$–K^+	0.102	−0.267	0.349	0.102	−0.190	0.176	0.112	−0.144	0.092	0.112	−0.139	0.086
13. Borazine–$(NO_2)_3$	0.095	−0.240	0.303	0.095	−0.235	0.290	0.098	−0.230	0.269	0.098	−0.229	0.267
14. Borazine–$(NO_2)_3$–Li^+	0.087	−0.369	0.782	0.087	−0.297	0.506	0.095	−0.245	0.315	0.096	−0.240	0.3
15. Borazine–$(NO_2)_3$–Na^+	0.087	−0.379	0.825	0.087	−0.301	0.520	0.094	−0.244	0.316	0.094	−0.239	0.303
16. Borazine–$(NO_2)_3$–K^+	0.088	−0.358	0.728	0.088	−0.291	0.481	0.094	−0.246	0.321	0.094	−0.241	0.308

influenced by their interaction with alkali metal cations, their reactivity can be further enhanced by substitution with EDGs or EWGs and finally their reactivity trend is altered depending on the polarity of the solvent used.

To investigate the effect of the basis set we calculated values of η, μ and ω for benzene and borazine complexes at the B3LYP/6-31++G(d,p) and the B3LYP/6-311++G(d,p) level of theory. The increase in the basis set size hardly affects the chemical reactivity values (Tables S6 and S7†). The electrophilicity index (ω) of borazine cation–π complexes correlates well with the binding energy value obtained in the gas phase and in the solvent phase (benzene), Fig. 7. This further implies

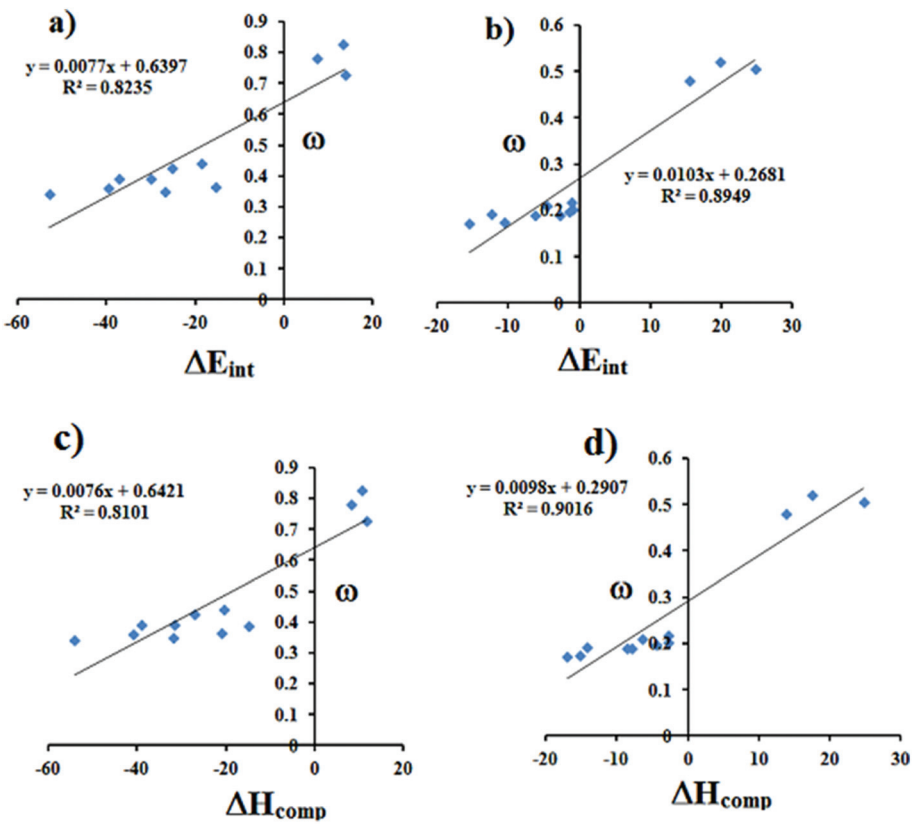

Fig. 7 Correlation plot between the interaction energies (X-axis) of various substituted cation–π complexes of borazine and electrophilicity index, ω (Y-axis) in (a) the gas phase and (b) benzene medium. (c) and (d) show the correlation of the enthalpy of complexation (ΔH_{comp}) with electrophilicity (ω) in the gas and solvent phase (benzene).

that any change in the interaction energy of the cation–π complex will influence the chemical reactivity of the aromatic systems.

Thermochemical analysis

To examine the thermodynamic driving force involved in the complex formation we performed thermochemical analysis. The enthalpy of complexation calculated in the gas phase and in three different solvent phases *viz.* benzene, acetone and water, are depicted in Table 10. The higher negative value of enthalpy of complexation (ΔH_{comp}) in the gas phase indicates that the complexation process is exothermic in nature and that a strong thermodynamic driving force for the cation–π complexation exists. In the case of the cation–π complex of benzene in the gas phase, ΔH_{comp} is observed to be in the order, −36.93 (Li^+) > −24.12 (Na^+) > −17.48 (K^+) (values are in kcal mol^{-1}). Strong inverse dependence of ΔH_{comp} on the size of the cation is observed. This observed trend can be related to the polarizing ability of a cation by the anion (here the π-electron cloud). Since Li^+ is comparatively smaller than Na^+ or K^+, it is highly polarized by the π-electron cloud resulting in a greater negative value of ΔH_{comp}. The presence of the electron donation groups, $-CH_3$ and $-NH_2$ are also found to influence ΔH_{comp} and this influence is greatest in $-NH_2$ substituted benzene. Similar trends in the magnitude of the gas phase enthalpy in the case of borazine substituted compounds are also observed, Table 10. However, complexes with borazine are less exothermic compared to benzene substituted compounds. On the other hand, the presence of EWGs, $-NO_2$, makes the complexation endothermic. Even though the gas phase complexations are highly exothermic, a spiky fall in the values is observed upon introduction of the solvent phases. In benzene medium, ΔH_{comp} values are in the range of −5.99 kcal mol^{-1} to −19.19 kcal mol^{-1} and for borazene compounds with EDG these values range from −2.73 kcal mol^{-1} to −17.00 kcal mol^{-1}. Table 10 denies the presence of any thermodynamic driving forces for the complexation with nitro-substituted borazines and the reaction is observed to be endothermic for all three cations. Of the three cations, K^+ shows the highest values. On increasing the solvent polarity, in the acetone and water phases, ΔH_{comp} became endothermic in most cases, Table 10. Therefore, solvent polarity plays a negative role on the complex formation. Interestingly, K^+ complexes are observed to be exothermic with a very small negative ΔH_{comp} in the aqueous phase, Table 10. From the above discussion, it can be construed that the solvent polarity and EWD groups play a negative role on the thermodynamic driving force for complexation. The ΔH_{comp} values of borazine cation–π complexes are found to have a good correlation ($R^2 > 0.90$, Fig. 7) with the electrophilicity index (ω) both in the gas and solvent phases (benzene) indicating a dependency of the reactivity of such complexes on the enthalpy of complexation.

Table 10 Enthalpy of complexations (ΔH_{comp}) in four different phases at the MP2/6-31+G(d) level of theory

	ΔH_{comp} (in kcal mol^{-1})			
Systems	Gas	Benzene	Acetone	Water
Benzene–Li^+	−36.93	−8.39	8.33	9.49
Benzene–Na^+	−24.12	−5.99	3.45	4.07
Benzene–K^+	−17.48	−6.79	−1.16	−0.78
Benzene–$(CH_3)_3$–Li^+	−44.22	−11.74	7.23	8.51
Benzene–$(CH_3)_3$–Na^+	−29.18	−8.22	2.56	3.25
Benzene–$(CH_3)_3$–K^+	−23.33	−10.76	−3.48	−3.08
Benzene–$(NH_2)_3$–Li^+	−53.64	−19.19	4.56	7.17
Benzene–$(NH_2)_3$–Na^+	−38.76	−15.08	0.74	2.19
Benzene–$(NH_2)_3$–K^+	−32.88	−16.75	−4.81	−3.63
Borazine–Li^+	−31.77	−2.83	13.10	14.22
Borazine–Na^+	−20.47	−2.78	6.24	6.83
Borazine–K^+	−15.03	−4.50	1.00	1.37
Borazine–$(CH_3)_3$–Li^+	−41.04	−7.93	9.65	11.62
Borazine–$(CH_3)_3$–Na^+	−27.25	−6.48	3.48	4.86
Borazine–$(CH_3)_3$–K^+	−21.00	−8.61	−2.09	−0.99
Borazine–$(NH_2)_3$–Li^+	−54.19	−17.00	7.16	9.23
Borazine–$(NH_2)_3$–Na^+	−39.19	−14.29	2.11	3.53
Borazine–$(NH_2)_3$–Na^+	−32.06	−15.23	−3.27	−2.13
Borazine–$(NO_2)_3$–Li^+	8.30	24.85	26.46	25.82
Borazine–$(NO_2)_3$–Na^+	10.66	17.49	13.64	12.62
Borazine–$(NO_2)_3$–K^+	11.63	13.90	9.48	8.63

Conclusion

The importance of the cation–π interaction increases day by day due to its recognition in many areas of chemistry. Its significance has been highlighted in various fields of chemistry from biology to macromolecular chemistry to drug receptor chemistry. In this study, quantum chemical calculations have been carried out on the cation–π complexes of benzene and its inorganic analogue, borazine. In cationic complexes of benzene, all the benzene rings adopt a planar geometry and η^6 coordination mode. However, all the borazine rings in their cationic complexes adopt a puckered structure and η^3 coordination mode. Remarkably, despite this non-planar geometry, all the B–N bond lengths are equal. This is due to the fact that non-planar borazine rings have a higher degree of π electron delocalization compared with the planar rings. This has been further confirmed at different levels of theory as well as by topological analysis which revealed that the ellipticity of the B–N bonds increases in the non-planar geometry. Topological analysis revealed that the interaction between the cation and the ring π cloud is electrostatic in nature. The strength of such interactions increases as electron donating substituents such as $-CH_3$ and $-NH_2$ are attached to the rings, while electron withdrawing substituents such as $-NO_2$ decrease the interaction strength. The calculated binding energy has been found to correlate well with the force constant of the bond between the metal cation and the ring, as well as with the charge transfer values. The correlation between the Hammett constants and the interaction energies implies that both induction and resonance effects contribute to the cation–π interaction. The discrete solvation model suggests that the interaction energy within borazine–cation–π complexes increases with increasing numbers of water molecules. In conclusion, this study reveals that like benzene, borazine–cation complexes have a

significant binding energy which increases with the addition of electron donating substituents while electron withdrawing substituents decrease it. Thermochemical analysis confirmed that in the gas phase, the complexation is enthalpy driven, whereas the polarity of the solvent and the EWD group, $-NO_2$, impart a negative role on the thermochemistry of the complexation reaction. Furthermore, due to the cation–π interaction the chemical reactivity values change. It was found that complexes associated with larger cations have a minimum value of η and μ and a maximum value of ω and therefore have a higher reactivity in comparison to benzene and borazine.

Computational details

All cation–π complexes are initially subjected to geometry optimization at the B3LYP/6-31+G(d) level of theory without any symmetry constraints.[60] To observe the effect of the basis set we carried out single point calculations at the B3LYP/6-31++G(d,p), and B3LYP/6-311++G(d,p) levels of theory. To observe consistency in the results of B3LYP and MP2 calculations, we further optimized the geometries at the MP2/6-31+G(d) level of calculation, and single point calculations were performed at MP2/6-31++G(d,p) and MP2/6-311++G(d,p) levels of theory. The nature of the stationary points was confirmed by frequency calculations at the same level of theory. All the structures are found to be at local minima on the potential energy surface as their respective Hessian (matrix of analytically determined second derivative of energy) was real. Interaction energies obtained using the above mentioned levels of theory have been corrected for basis set superposition error (BSSE) with the "Counterpoise = N" option for all fragments in the complex using the Boys and Bernardi's counterpoise method.[61] Natural bond orbital (NBO)[62] analysis was also carried out at the same level of theory. The strengths of individual bonds were ascertained from their Wiberg bond index (WBI)[62c] values available within the NBO routine. To examine the effect of the solvent on the thermodynamics of the complexation reaction, we assigned three solvents, ranging from non-polar to polar: benzene, acetone and water. Solvation effects are included by means of the polarizable continuum model (PCM).[63] The discrete solvation model at the B3LYP/6-31++G(d,p) level were performed in borazine cation–π complexes with up to five water molecules. All the calculations were performed using Gaussian 09 programs.[64]

Furthermore, to achieve an in-depth understanding of the bonding situation, topological analysis of the electron density $\rho(r)$ was carried out within the realm of quantum theory of atoms in molecules (QTAIM).[35] This was done by first generating the wavefunction file using the keyword DENSITY = CURRENT in Gaussian 09 and then analyzed using the AIMPAC[65] and AIMALL[66] suite of programs. Nucleus independent chemical shift (NICS) calculations for the planar rings were calculated by placing a ghost atom (symbol Bq) at the geometric mean of the ring (designated as NICS(0)) and at 1 Å above the ring (designated as NICS(1)) at the B3LYP/6-31+G(d) level of theory.

Interaction energies were calculated using a super molecular approach ($[\Delta E_{int} = (E_{B-cat}) - (E_B + E_{cat})]$, where, E_{B-cat} is the energy of the complex, E_B is the energy of benzene or borazine and E_{cat} is the energy of the cation). Thermochemical analysis was performed to examine the thermodynamic driving forces for the complexation reactions in the gas as well as the solvent phase. Apart from that, we made DFRT (density functional reactivity theory) studies to quantify the chemical stability of the complexes. Under DFRT, the chemical potential (μ) and global hardness (η) can be expressed in terms of finite difference approximation[67] and Koopman's approximation[68] as,

$$\eta = \frac{(\mathrm{IP} - \mathrm{EA})}{2} = \frac{E_{\mathrm{LUMO}} - E_{\mathrm{HOMO}}}{2},$$

$$\mu = \frac{(\mathrm{IP} - \mathrm{EA})}{2} = \frac{E_{\mathrm{LUMO}} - E_{\mathrm{HOMO}}}{2}.$$

The global electrophilicity index (ω) as introduced by Parr *et al.*[69] can be defined as

$$\omega = \frac{\mu^2}{2\eta}.$$

These are extremely useful parameters to follow the chemical reactivity of a species and a number of studies witnessed its applicability.[70] Herein, we have calculated chemical hardness (η), chemical potential (μ) and electrophilicity index (ω) values of the benzene/borazene–cation complexes to examine their chemical reactivity.

Acknowledgements

The authors thank Prof. M. K. Chaudhuri, Vice Chancellor, Tezpur University for the financial support.

Notes and references

1 S. E. Wheeler, *Acc. Chem. Res.*, 2013, **46**, 1029–1038.
2 R. Wu and T. B. McMahon, *J. Am. Chem. Soc.*, 2008, **130**, 12554–12555.
3 C. A. Deakyne and M. Meot-Ner, *J. Am. Chem. Soc.*, 1985, **107**, 474–479.
4 M. Meot-Ner and C. A. Deakyne, *J. Am. Chem. Soc.*, 1985, **107**, 469–474.
5 D. A. Dougherty, *Science*, 1996, **271**, 163–168.
6 J. C. Ma and D. A. Dougherty, *Chem. Rev.*, 1997, **97**, 1303–1324.
7 A. McCurdy, L. Jimenez, D. A. Stauffer and D. A. Dougherty, *J. Am. Chem. Soc.*, 1992, **114**, 10314–10321.
8 J. P. Gallivan and D. A. Dougherty, *Proc. Natl. Acad. Sci. U. S. A.*, 1999, **96**, 9459–9464.

9 J. Sunner, K. Nishizawa and P. Kebarle, *J. Phys. Chem.*, 1981, **85**, 1814–1820.
10 D. Kim, S. Hu, P. Tarakeshwar and K. S. Kim, *J. Phys. Chem. A*, 2003, **107**, 1228–1238.
11 P. Lakshminarasimhan, R. B. Sunoj, J. Chandrasekhar and V. Ramamurthy, *J. Am. Chem. Soc.*, 2000, **122**, 4815–4816.
12 C. D. Sherrill, *Acc. Chem. Res.*, 2013, **46**, 1020–1028.
13 N. Zacharia and D. A. Dougherty, *Trends Pharmacol. Sci.*, 2002, **23**, 281–287.
14 N. S. Scrutton and A. R. Raine, *Biochem. J.*, 1996, **319**, 1–8.
15 D. L. Beene, G. S. Brandt, W. G. Zhong, N. M. Zacharias, H. A. Lester and D. A. Dougherty, *Biochemistry*, 2002, **41**, 10262–10269.
16 X. Xiu, N. L. Puskar, J. A. P. Shanata, H. A. Lester and D. A. Dougherty, *Nature*, 2009, **458**, 534–537.
17 K. Brejc, W. J. van Dijk, R. V. Klaassen, M. Schuurmans, J. van Der Oost, A. B. Smit and T. K. Sixma, *Nature*, 2001, **411**, 269–276.
18 D. A. Dougherty, *Acc. Chem. Res.*, 2013, **46**, 885–893.
19 K. E. Riley and P. Hobza, *Acc. Chem. Res.*, 2013, **46**, 927–936.
20 S. Yamada and J. S. Fossey, *Org. Biomol. Chem.*, 2011, **9**, 7275–7281.
21 Y. Mori and S. Yamada, *Molecules*, 2012, **17**, 2161–2168.
22 S. Yamada, *Org. Biomol. Chem.*, 2007, **5**, 2903–2912.
23 R. A. Kumpf and D. A. Dougherty, *Science*, 1993, **261**, 1708–1710.
24 C. A. Hunter, *Angew. Chem., Int. Ed.*, 2004, **43**, 5310–5324.
25 M. F. Rasekh, *Struct. Chem.*, 2012, DOI: 10.1007/s11224-012-9954-9.
26 R. Miao, G. Yang, C. Zhao, J. Hong and L. Zhu, *J. Mol. Struct. (THEOCHEM)*, 2005, **715**, 91–100.
27 J. E. Huheey, A. E. Keiter and R. L. Keiter, *Inorganic Chemistry: Principle of Structure and Reactivity*, Harper Collins College Publishers, New York, 1993.
28 S. A. Arnstein and C. D. Sherrill, *Phys. Chem. Chem. Phys.*, 2008, **10**, 2646–2655.
29 M. O. Sinnokrot and C. D. Sherrill, *J. Am. Chem. Soc.*, 2004, **126**, 7690–7697.
30 M. O. Sinnokrot and C. D. Sherrill, *J. Phys. Chem. A*, 2003, **107**, 8377–8379.
31 A. S. Mahadevi and G. N. Sastry, *Chem. Rev.*, 2013, **113**, 2100–2138.
32 A. K. Phukan, A. K. Guha and B. Silvi, *Dalton Trans.*, 2010, **39**, 4126–4137.
33 J. B. Nicholas, B. P. Hay and D. A. Dixon, *J. Phys. Chem. A*, 1999, **103**, 1394–1400.
34 (*a*) A. Schaefer, H. Horn and R. Ahlrichs, *J. Chem. Phys.*, 1992, **97**, 2571–2577; (*b*) T. H. Dunning Jr., *J. Chem. Phys.*, 1989, **90**, 1007–1023.
35 R. W. F. Bader, *Atoms in Molecules: a Quantum Theory*, Oxford University Press, Oxford, U. K., 1990.
36 J. S. Rao, H. Zipse and G. N. Sastry, *J. Phys. Chem. B*, 2009, **113**, 7225–7236.
37 R. A. Kumpf and D. A. Dougherty, *Science*, 1993, **261**, 1708–1710.
38 J. Cheng, Z. Gong, W. Zhu, Y. Tang, W. Li, Z. Li and H. Jiang, *J. Phys. Org. Chem.*, 2007, **20**, 448–453.
39 D. Kim, S. Hu, P. Tarakeshwar, K. S. Kim and J. M. Lisy, *J. Phys. Chem. A*, 2003, **107**, 1228–1238.
40 M. S. Marshall, R. P. Steele, K. S. Thanthiriwatte and C. D. Sherrill, *J. Phys. Chem. A*, 2009, **113**, 13628–13632.
41 N. J. Singh, S. K. Min, D. Y. Kim and K. S. Kim, *J. Chem. Theory Comput.*, 2009, **5**, 515–529.
42 L. K. Engerer and T. P. Hanusa, *J. Org. Chem.*, 2011, **76**, 42–49.
43 (*a*) A. S. Reddy, H. Zipse and G. N. Sastry, *J. Phys. Chem. B*, 2007, **111**, 11546–11553; (*b*) C. Adamo, G. Berthier and R. Savinelli, *Theor. Chem. Acc.*, 2004, **111**, 176–181; (*c*) Y. Xu, J. Shen, W. Zhu, X. Luo, K. Chen and H. Jiang, *J. Phys. Chem. B*, 2005, **109**, 5945–5949.
44 L. P. Hammett, *J. Am. Chem. Soc.*, 1937, **59**, 96–103.
45 S. E. Wheeler and K. N. Houk, *J. Am. Chem. Soc.*, 2008, **130**, 10854–10855.
46 F. Cozzi, M. Cinquini, R. Annunziata, T. Dwyer and J. Siegel, *J. Am. Chem. Soc.*, 1992, **114**, 5729–5733.
47 M. Lewis, C. Bagwill, L. K. E. Hardebeck and S. Wireduaah, *Comput. Struct. Biotechnol. J.*, 2012, **1**, 1–9.
48 S. Mecozzi, A. P. West and D. A. Dougherty, *J. Am. Chem. Soc.*, 1996, **118**, 2307–2308.
49 Z. Weiliang, X. Tan, J. Shen, X. Luo, F. Cheng, P. C. Mok, R. Ji, K. Chen and H. Jiang, *J. Phys. Chem. A*, 2003, **107**, 2296–2303.
50 J. Poater, I. Garcia-Cruz, F. Illas and M. Sola, *Phys. Chem. Chem. Phys.*, 2004, **6**, 314–318.
51 E. D. Jemmis and B. Kiran, *Inorg. Chem.*, 1998, **37**, 2110–2116.
52 I. Alkorta, I. Rozas and J. Elguero, *J. Am. Chem. Soc.*, 2002, **24**, 8593–8598.
53 A. Saieswari, U. D. Priyakumar and G. N. Sastry, *J. Mol. Struct. (THEOCHEM)*, 2003, **663**, 145–148.
54 D. Vijay, H. Zipse and G. N. Sastry, *J. Phys. Chem. B*, 2008, **112**, 8863.
55 D. Vijay and G. N. Sastry, *Chem. Phys. Lett.*, 2010, **485**, 235.
56 G. A. Jeffrey, *An Introduction to Hydrogen Bonding*, Oxford University Press, New York, 1997.
57 R. G. Parr and P. K. Chattaraj, *J. Am. Chem. Soc.*, 1991, **113**, 1854–1855.
58 K. K. Bania, D. Bharali, B. Viswanathan and R. C. Deka, *Inorg. Chem.*, 2012, **51**, 1657–1674.
59 P. Sarmah and R. C. Deka, *Int. J. Quantum Chem.*, 2008, **108**, 1400–1409.
60 (*a*) C. Møller and M. S. Plesset, *Phys. Rev.*, 1934, **46**, 618–622; (*b*) J. S. Binkley and J. A. Pople, *Int. J. Quantum Chem.*, 1975, **9**, 229–236.
61 S. F. Boys and R. Bernardi, *Mol. Phys.*, 1979, **19**, 553–566.
62 (*a*) E. D. Glendening, A. E. Reed, J. E. Carpenter and F. Weinhold, *NBO Program 3.1*, University of Wisconsin, Madison, WI, 1988; (*b*) A. E. Reed, F. Weinhold and L. A. Curtiss, *Chem. Rev.*, 1988, **88**, 899–926; (*c*) K. B. Wiberg, *Tetrahedron*, 1968, **24**, 1083–1096.

63 (*a*) V. Barone and M. Cossi, *J. Phys. Chem. A*, 1998, **102**, 1995–2001; (*b*) M. Cossi, N. Rega, G. Scalmani and V. Barone, *J. Comput. Chem.*, 2003, **24**, 669–681.

64 M. C. Frisch, *et al.*, *Gaussian 09, revision A.1*, Gaussian, Inc., Wallingford, CT, 2009; M. J. Frisch, G. W. Trucks, H. B. Schlegel, G. E. Scuseria, M. A. Robb, J. R. Cheeseman, G. Scalmani, V. Barone, B. Mennucci, G. A. Petersson, H. Nakatsuji, M. Caricato, X. Li, H. P. Hratchian, A. F. Izmaylov, J. Bloino, G. Zheng, J. L. Sonnenberg, M. Hada, M. Ehara, K. Toyota, R. Fukuda, J. Hasegawa, M. Ishida, T. Nakajima, Y. Honda, O. Kitao, H. Nakai, T. Vreven, J. A. Montgomery Jr., J. E. Peralta, F. Ogliaro, M. Bearpark, J. J. Heyd, E. Brothers, K. N. Kudin, V. N. Staroverov, R. Kobayashi, J. Normand, K. Raghavachari, A. Rendell, J. C. Burant, S. S. Iyengar, J. Tomasi, M. Cossi, N. Rega, J. M. Millam, M. Klene, J. E. Knox, J. B. Cross, V. Bakken, C. Adamo, J. Jaramillo, R. Gomperts, R. E. Stratmann, O. Yazyev, A. J. Austin, R. Cammi, C. Pomelli, J. W. Ochterski, R. L. Martin, K. Morokuma, V. G. Zakrzewski, G. A. Voth, P. Salvador, J. J. Dannenberg, S. Dapprich, A. D. Daniels, O. Farkas, J. B. Foresman, J. V. Ortiz, J. Cioslowski and D. J. Fox, *GAUSSIAN 09 (Revision A.1)*, Gaussian, Inc., Wallingford, CT, 2009.

65 R. F. W. Bader, *AIMPAC*, http://www.chemistry.mcmaster.ca/aimpac/

66 T. A. Keith, *AIMAll (Version 13.02.26, Professional)*, 2013, http://aim.tkgristmill.com

67 R. G. Parr and W. Yang, *Density Functional Theory of Atoms and Molecules*, Oxford University Press, New York, 1989.

68 T. A. Koopmans, *Physica*, 1933, **1**, 104–113.

69 R. G. Parr, L. Szentpaly and S. Liu, *J. Am. Chem. Soc.*, 1999, **121**, 1922–1924.

70 (*a*) K. K. Bania and R. C. Deka, *J. Phys. Chem. C*, 2011, **115**, 9601–9607; (*b*) K. K. Bania and R. C. Deka, *J. Phys. Chem. C*, 2013, **117**, 11663–11678.

